TENTH INTERNATIONAL CONFERENCE ON NON-CONVENTIONAL MATERIALS AND TECHNOLOGIES

NOCMAT 2008

Cali, Colombia. 12-14 November, 2008

EFFECT OF NATURAL WEATHERING ON POROSITY AND MINERAL COMPOSITION OF CEMENTITIOUS ROOFING TILES REINFORCED WITH FIQUE FIBRE

G. H. D. Tonoli[1], S. F. Santos[2], H. Savastano Jr.[2], S. Delvasto[3], R. Mejía de Gutiérrez[3], M. del M. Lopez de Murphy[4]

[1]Escola de Engenharia de São Carlos, Universidade de São Paulo, Brazil

[2]Faculdade de Zootecnia e Engenharia de Alimentos, Universidade de São Paulo, Brazil. E-mail:holmersj@usp.br

[3]Escuela de Ingeniería de Materiales, Grupo de Materiales Compuestos, Universidad del Valle, Colombia.

[4]Civil and Environmental Engineering Department, Penn State University, mmlopez@engr.psu.edu

ABSTRACT

The objective of the present work was to evaluate the effects of 14 years of weathering exposition to tropical conditions on the porosity and mineral composition of cementitious roofing tiles (corrugated sheets), still in service, reinforced with fique fibres (*Furcrae gender*). The matrix of the roofing tiles consisted of Type I Portland

cement, lime and river sand in the following proportion 1:0.1:2 (by weight) and a water-cement ratio of 0.5. The corrugated sheets were cast by hand followed by compaction of the fresh tiles on a vibrating table. Water absorption, apparent void volume, bulk density, porosity by mercury intrusion, thermogravimetric analyses and air permeability evaluated by Forchheimer's equation were determined. X-ray diffraction was performed in order to achieve mineral composition of the tiles aged in laboratory and under exposition to natural weathering. The results show that tiles under weathering exposition presented higher water absorption and apparent void volume than tiles under laboratory exposition. The continuous hydration of cement and natural carbonation filled the smaller pores (below 100 nm) but contrarily the large pores remained in the matrix, what increased the value of the average pore diameter of the composite under natural weathering. On the other hand, its microstructure presented lower air permeability than tiles aged in laboratory. It is reasonable to suppose that in the weathering exposed tiles the low quantity of permeable porous and the increase of apparent void volume were caused by the combined effects of continuous hydration and carbonation as well as because of the surface leaching process, respectively. Besides, in the weathering aged tiles it seemed to take place a more intensive hydration process as it was identified greater amount of hydrated phases by X-ray diffraction patterns than in the laboratory aged specimens.

Keywords: air permeability, Fique fibres, durability, cementitious corrugated sheets, vegetable fibres, Forchheimer's equation.

INTRODUCTION

Since ancient times, approximately 3500 years ago, brittle building materials, e.g. clay sun baked bricks, were reinforced with vegetable fibres. However, the concept of vegetable fibre reinforcement in cement-based materials was developed in decade 1970's, when vegetable fibres were evaluated as substitutes of man-made fibres and asbestos fibres [1,2]1. Natural vegetable fibres (cellulose pulp, sisal, bamboo, fique, hemp, flax, jute and ramie, for example) are used in those countries where these fibres are easily available. The developing societies have to look for alternative and local raw materials. For this reason, in cement based composites, many types of vegetable fibres are used in order to decrease costs and to satisfy increasing demands of sustainability and ecology.

Structural elements with vegetable fibres are important for construction of inexpensive buildings in developing regions of the world, on the contrary, the use of synthetic fibres frequently involve higher costs and great consumption of energy in the processing of fiber reinforced cementitious composites [3]. According to Swamy [4], the use of composites reinforced with vegetable fibres in flat sheets, roofing tiles and pre-manufactured components can represent significant contribution to the infrastructure in developing countries. It has been demonstrated that fique fibre, which is a commercially available natural fibre in Colombia, is appropriate for low cost housing applications when incorporated into a matrix based on Portland cement, being suitable for making elements of various shapes using simple production processes [5,6]. Another concern is the durability of alternative products, as well as their compatibility to the service life of the components destined to buildings of low income population [7].

The present study was carried out to evaluate the microstructure properties and chemical composition of tiles reinforced with lignocellulosic fibres and exposed during 14 years under laboratory and weathering conditions.

EXPERIMENTAL

Characteristics of the fique fibres

Fique fibre or cabuya (Furcrae gender) is a Colombian native vegetable fibre with similar characteristics to sisal. It has been demonstrated that the fique fibre is suitable for cementitious materials in low cost housing applications [5,6,8] and for fibre reinforcement of concrete [9].

Figure 1 shows scanning electron micrographs (SEM) of the fique fibres. The fibres thickness is more than 0.2 mm (Figure 1a). In the outer wall (primary wall) the fibrillae have a reticulated structure (Figure 1b). The fibre consists of a number of walls built up of fibrillae. The fibrilllae are, in turn, built up of microfibrillae. The microfibrillae are composed of cellulose molecular chains with thickness of few micrometers (approximately 4 μm) as seen in Figures 1c and 1d.

A fique fibre in cross section is built up of about many fibre cells (each with 3-4 μm of diameter). The fibre cells are linked together by means of lamellae, which consist of hemicelluloses, lignin and pectin (Figures 1c and 1d).

The properties of the fibres are listed in Table 1.

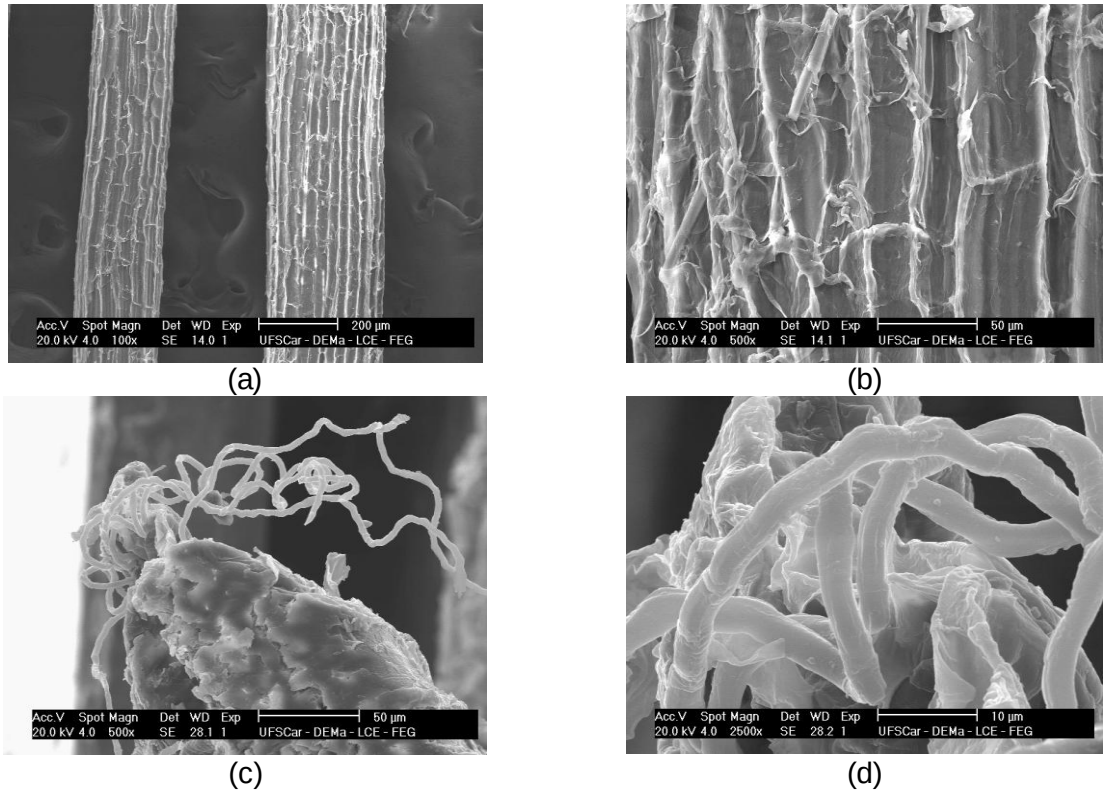

FIGURE 1 – SCANNING ELECTRON MICROGRAPHS OF THE FIQUE FIBRES. THE FIBRE IS BUILT UP OF FIBRE CELLS LINKED EACH OTHER BY MEANS OF THE MIDDLE LAMELLAE (A AND B). APPROXIMATELY 4 µM LOOSE FILAMENTS OR MICROFIBRILLAE (C AND D).

TABLE 1 – CHARACTERISTICS OF THE FIQUE FIBRES [10].

Property	Range	Average
Thickness (mm)	0.17 - 0.29	0.23
Apparent density (g/cm^3)	0.678 - 0.767	0.723
Real density (g/cm^3)	-	1.47
Fibre fineness, Tex (weight in grams of 1000 meters of yarn)	25.2 - 58.3	44.2
Water absorption (%)	-	60
Non fibrous material (%)	0.06 - 0.16	0.10
Ash (%)	-	0.58
Lignin (%)	-	10.1
Cellulose (%)	-	70.0
Modulus of elasticity (GPa)	-	8.2
Tensile strength (MPa)	324 - 688	537

Production of the roofing tiles

The matrix of the roofing tiles used in this study consisted of ordinary Portland cement, lime and river sand in the following proportion 1:0.1:2 ((by weight). The water-cement ratio was 0.5. The fibres were cut to the desired average length of 20 mm and used as 3% of the total mass of solids. Tiles were exposed during 14 years under laboratory and weathering conditions at Cali, Colombia. Despite being **exposed** to the **weather** there is no visible sign of decay in the corrugated sheets, which have been mounted on a small prototype house roof structure. Until now, the roof stability and form are maintained.

Microstructure characterization tests

Tiles of each condition were evaluated on permeability properties (porosity and air permeability) and chemical composition. Water absorption (WA), apparent void volume (AVV) and bulk density (BD) results were obtained under 2 h vacuum (~80 KPa gauge) after 24 h immersed in tap water. Real density was measured using a Quantachrome multipicnometer, model MVP-6DC.

Mercury intrusion porosimetry (MIP) was performed using Micrometrics 9320 Poresizer with operation pressures of up to 200 MPa. The assumptions were 0.000495 kg/cm^2 mercury surface tension and 13.5335 kg/m^3 mercury density. Equilibration time in both low and high pressure was 10 s. The advancing/receding contact angle was assumed to be 130°. The amount of mercury introduced at each pressure interval was recorded. Specimens were cut with a cubic side length of approximately 5 mm, dried at 70^{o}C for 24 h and stored in an air-tight recipient prior to evaluation. Sample weight was approximately 2 g. The technique was adopted in order to evaluate the pore size distribution as usually applied in the characterization of cement based materials [11,12,13].

Experimental evaluation of air permeability at room temperature (25 – 30^{o}C) was conducted in a permeameter, as described by Innocentini et al. [14]. The sample was fixed between two chambers with a testing area of 4.91 x 10^{-4} m^2. The experiments evaluated the easiness of airflow passing through the sample thickness (around 8 mm) by measuring the exit air velocity in response to the variations of the inlet pressure applied. Permeability tests were performed on at least three specimens for each treatment. Samples were previously dried in a ventilated oven at 100^{o}C. The moisture was removed primarily to prevent any influence of water on the

measurements. The permeability constants k_1 and k_2 were obtained by fitting the experimental data using Forchheimer's equation (Eq.1), expressed for flow of compressible fluids [15]:

$$\frac{P_i^2 - P_o^2}{2P_o L} = \left(\frac{\mu}{k_1}\right) v_s + \left(\frac{\rho}{k_2}\right) v_s^2 \qquad (1)$$

Where P_i and P_o are the absolute inlet and outlet air pressures respectively; v_s is the fluid velocity; L the sample thickness; μ the fluid viscosity (air viscosity ~1.8 x 10^{-5} Pa.s); and ρ the fluid density (air density ~1.08 kg/m^3). The parameters k_1 and k_2 are the Darcian and non-Darcian permeability constants respectively.

The permeability constant k_1, or Darcian constant, represents the viscous effect of the shearing (friction and interactions between fluid and porous media); the permeability constant k_2, or non-Darcian constant, reflects the tortuosity of the porous media when the shearing velocity is high [16]. The higher the k_1 and k_2 values, the higher the permeability of the porous media.

Phase characterization of the roofing tiles

The chemical phases present in the roofing tiles samples were analyzed by X-ray diffraction (XRD) in a Rigaku Rotoflex RU-200B equipment with horizontal goniometer, multipurpose camera and monochromator. The conditions of operation were voltage of 50 kV, electric current equal to 100 mA, velocity of 1 degree/min and step of 0.02 degree. Samples used in this analysis were ground and passed through 45 μm screen.

Thermogravimetric analyses were conducted with a Netzsch STA409 PG using a sample mass of approximately 1.0 g and nitrogen atmosphere (flow ratio = 60 mL/min), heating ratio of 10°C/min up to maximum temperature of 1000°C. Prior to testing, the samples were dried at 40°C under low pressure (60 kPa) during 24 h to remove any moisture.

RESULTS AND DISCUSSION

Permeability and Microstructure properties

It was observed a tendency of high real density associated to the tiles under natural weathering exposition (Table 2). This could be the consequence of the formation of additional crystalline cementitious phases.

TABLE 2 – REAL DENSITY OF THE GROUND TILES.

	Laboratory exposition	Weathering exposition
Real density (g/cm^3)	2.65 ± 0.01	2.70 ± 0.12

Table 3 presents the physical properties of the specimens from laboratory and natural weathering exposition. The increase of the water absorption and apparent void volume in the roofing tiles aged under natural weathering exposition could be the consequence of the leaching of some less stable cementitious products, which decreased the bulk density of the specimens. Similarly, the mercury intrusion data (Table 4) shows the lower bulk density and apparent (skeletal) density of the specimens from weathering exposition. Despite of the lower total pore area of the weathering exposed tile, the average pore diameter increased around 50% in relation to the tile aged in laboratory.

TABLE 3 – AVERAGE VALUES AND STANDARD DEVIATIONS FOR WATER ABSORPTION (WA), APPARENT VOID VOLUME (AVV) AND BULK DENSITY (BD) FROM SPECIMENS OF THE ROOFING TILES.

	Laboratory exposition	Weathering exposition
Water absorption (%)	11.6 ± 1.3	13.5 ± 0.2
Apparent void volume (%)	22.9 ± 2.1	25.6 ± 0.2
Bulk density (g/cm^3)	1.97 ± 0.04	1.89 ± 0.02

Figure 2 presents the pore size distribution curve of the specimens from laboratory and weathering exposition. The peak below 10 nm is related to the cement paste and the peaks between 100 nm and 1000 nm are capillary pores resulting from the manufacturing process. The number of voids inside the fibre strands and cellulose fibres in fibre-cement actively influences the peak between 100 nm and 1000 nm [17]. Weathering exposed tile revealed a coarsening of pores greater than 100 nm in comparison with the tile aged in laboratory. Coarsening has been associated to the SiO_2 (gel) formation during carbonation of C–S–H [18] and leaching of the cement matrix [19].

TABLE 4 – INTRUSION DATA SUMMARY FOR THE TILES.

	Laboratory exposition	Weathering exposition
Total intrusion volume (mL/g)	0.030 ± 0.004	0.032 ± 0.006
Total pore area (m^2/g)	4.7 ± 0.5	3.4 ± 1.2
Median pore diameter - volume (µm)	0.036 ± 0.001	0.115 ± 0.013
Median pore diameter – area (µm)	0.013 ± 0.001	0.013 ± 0.001
Average pore diameter – 4V/A (µm)	0.025 ± 0.001	0.038 ± 0.006
Bulk density (g/cm^3)	1.99 ± 0.01	1.93 ± 0.02
Apparent (skeletal) density (g/cm^3)	2.11 ± 0.02	2.06 ± 0.01
Porosity (%)	5.87 ± 0.64	6.07 ± 1.17

It was outlined in Figure 2 the incidence of greater pores in the region between 100 and 400 nm for the tiles under natural weathering exposition. This profile indicates to be caused by high water absorption and apparent void volume in the roofing tiles aged under weathering exposition presented above. Differences in the curve of the pore size distribution had been evidenced mainly for the pores below 100 nm. During the weathering exposition the continuous hydration of cement occurred, but led to the reduction of the matrix voids, natural carbonation filled the lower pores (below 100 nm) in the matrix and remained the large pores, which increase the value of average pore diameter as described by Mehta & Monteiro [13]. However the decrease of the porosity in this region (below 100 nm) was sufficient to affect the total porosity of the tiles, as indicated by AVV values in Table 2. Larger pores attributed to fibres (around 1000 and 2000 nm) were not significantly affected by the weathering exposition.

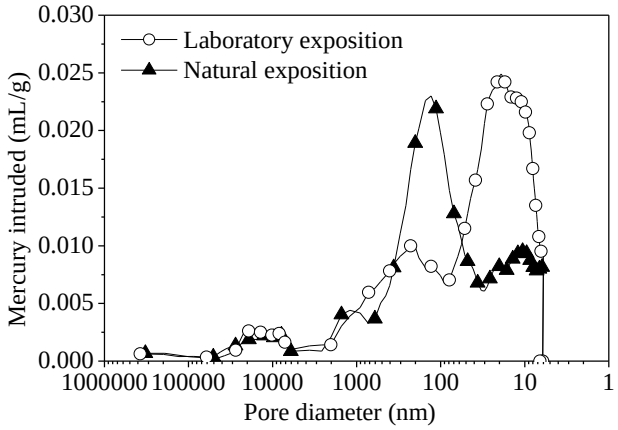

FIGURE 2 – PORE SIZE DISTRIBUTION FOR SPECIMENS AGED IN LABORATORY AND UNDER NATURAL WEATHERING EXPOSITION.

The air permeability is a physical property of extreme importance to the development of durable elements to civil construction. The permeability can be associated with the resistance to penetration of degradation agents and also with the microstructure properties (e.g. particle packing and permeable pores). In Figure 3 it can be observed that higher pressure is necessary to the same air velocity in the tiles aged under weathering exposition. Furthermore, the k_1 and k_2 values decreased in case of under natural weathering exposition in relation to laboratory exposition (Table 5). The decrease of k_1 indicates that friction and interactions between fluid and porous media increased. The non-Darcian constant, k_2, decreased in case of weathering exposition, which can signify the increase of the tortuosity of the porous structure.

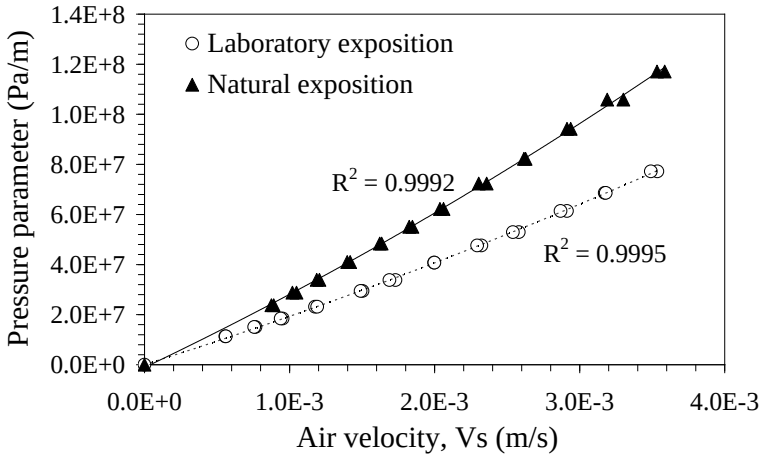

FIGURE 3 – FORCHHEIMER'S EQUATION FITTED TO EXPERIMENTAL DATA OF SPECIMENS AGED IN LABORATORY CONDITION AND UNDER NATURAL WEATHERING EXPOSITION ACCORDING TO THE EXPRESSION FOR COMPRESSIBLE FLUIDS.

TABLE 5 – DARCIAN (K_1) AND NON-DARCIAN (K_2) PERMEABILITY CONSTANTS OF THE TILES.

	k_1 (m^2)	k_2 (m)
Laboratory exposition	1.29E-15 ± 3.87E-16	1.97E-12 ± 1.25E-12
Weathering exposition	5.20E-16 ± 2.45E-16	4.90E-13 ± 1.59E-13

The primary cause of the change in the characteristics of a vegetable fibre in a cement based matrix is assumed by many researchers to be a chemical decomposition of the lignin and the hemicellulose, mainly in the middle lamella. The alkaline pore water in fibre-cement dissolves the lignin and the hemicelluloses. It can be seen in Figures 4a and 5a the link between the individual fibre cells. The long fique fibres can be broken down into numerous small units and loses its reinforcing

capacity in fibre-cement. It is generally held that decomposition of cellulose in an alkaline environment can take place in accordance with two different mechanisms. One is the peeling-off mechanism which occurs at the end of the molecular chain. The other form of cellulose decomposition is alkaline hydrolysis. This causes the molecular chains to divide, and the degree of polymerization decreases [20]. The the fibre cells can be filled with calcium hydroxide and the fibre loses its flexibility. It was not observed any constituents of pore water, for instance calcium hydroxide, in the cross-sectioned fique fibre and in an area close to it, according to energy dispersive X-ray spectroscopy (EDS) analysis (Figures 4b, 4c and 4d).

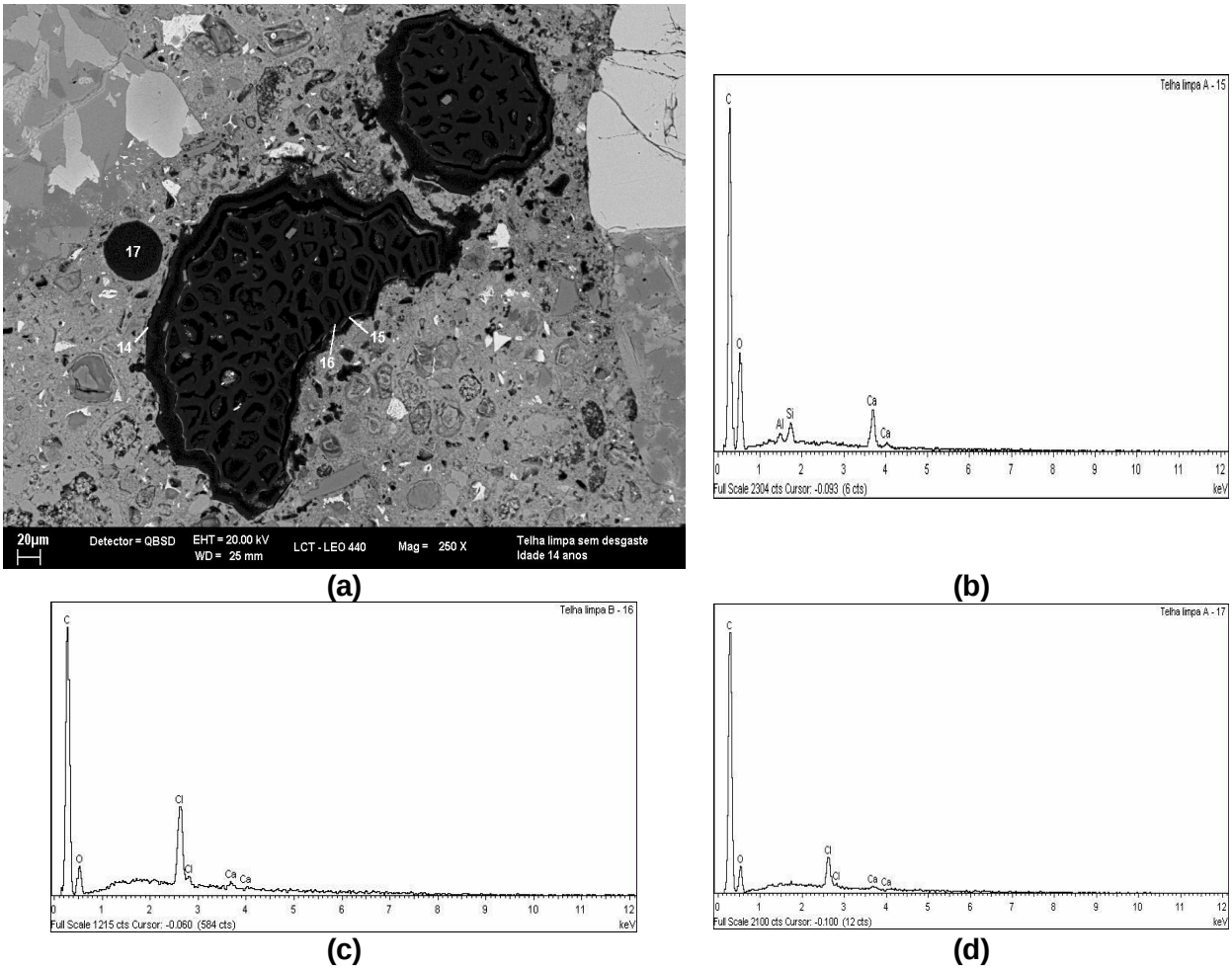

FIGURE 4 – BACK SCATTERING ELECTRONS (BSE) IMAGE OF THE CROSS-SECTIONED FIQUE FIBRE IN COMPOSITE OF 14 YEARS OLD, AGED IN LABORATORY. EDS SPOTS 15, 16 AND 17 AT FIBRE.

There is no evidence of difference of interface between the fibres and the matrix by scanning electron microscopy (SEM) micrographs of the tiles under laboratory and weathering exposition. On the other hand, after 14 years of continuous alternation of

wetting, heating, drying and carbonation, it can be supposed that there was some change in the chemical composition (for example, reduction of lignin, hemi-cellulose and cellulose content) mainly of the fibres of the tile under weathering exposition [21]. It can be seen in Figures 5b and 5d the energy dispersive X-ray spectroscopy (EDS) analysis indicating that fique fibre was slightly filled with Calcium. This result reflects slow carbonation during the weathering exposition.

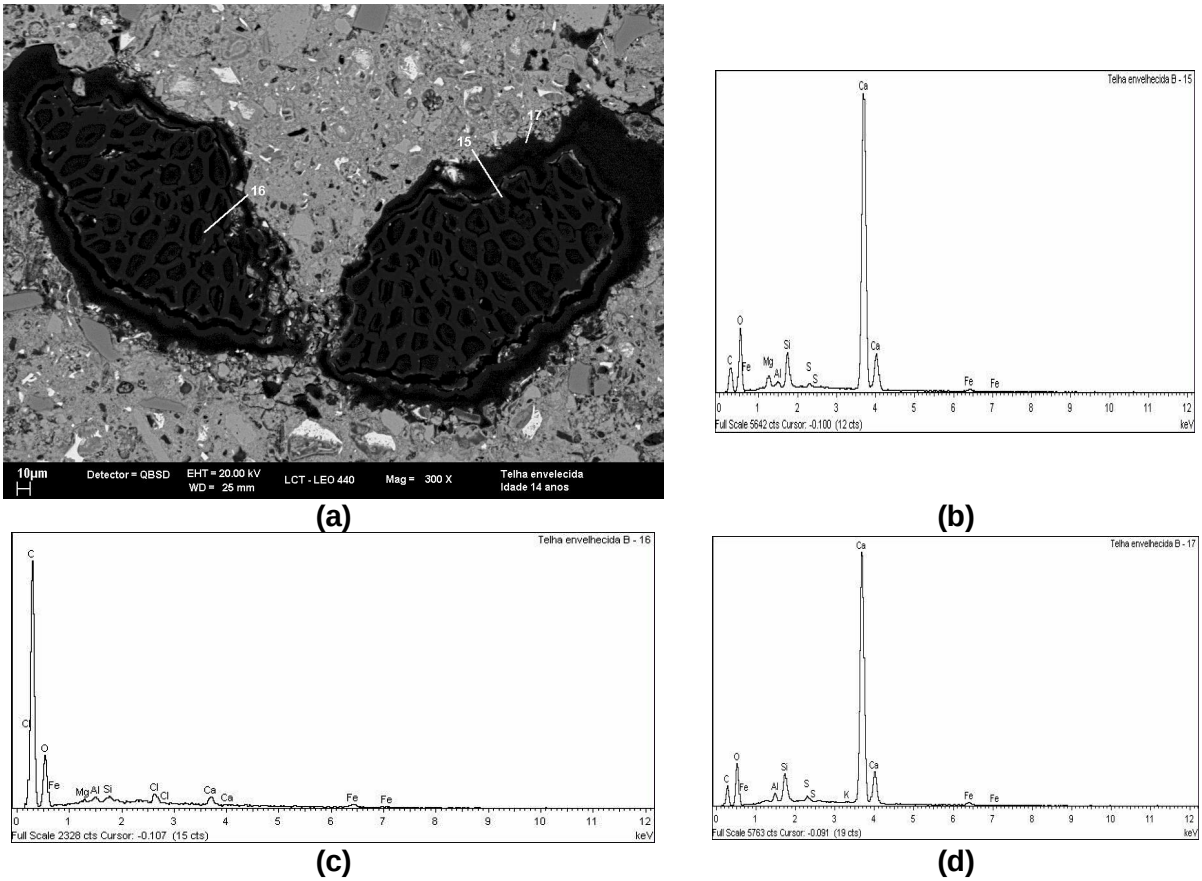

FIGURE 5 – BACK SCATTERING ELECTRONS (BSE) IMAGE OF THE CROSS-SECTIONED FIQUE FIBRE IN 14 YEARS OLD COMPOSITE, AGED UNDER NATURAL WEATHERING EXPOSITION. SPOTS 15 AND 16 AT LUMEN FIBRE; AND SPOT 17 AT FIBRE/MATRIX INTERFACE. THE SPOT 15 INDICATES HYDRATION PRODUCTS.

Figure 6 depicts the main cementitious phases present in the tiles aged in the laboratory. Other additional hydration products were identified in the tiles aged under weathering exposition (Figures 7), which can not be attributed to differences in the hydration process. Calcium hydroxide ($Ca(OH)_2$) was not identified in the tiles, regarding that 5% by mass is the limit of the equipment. Such a result indicates that in

the both tiles (in the laboratory and under weathering exposition) it was occurred the adsorption of CO_2 in the cement based matrix and formation of calcite ($CaCO_3$).

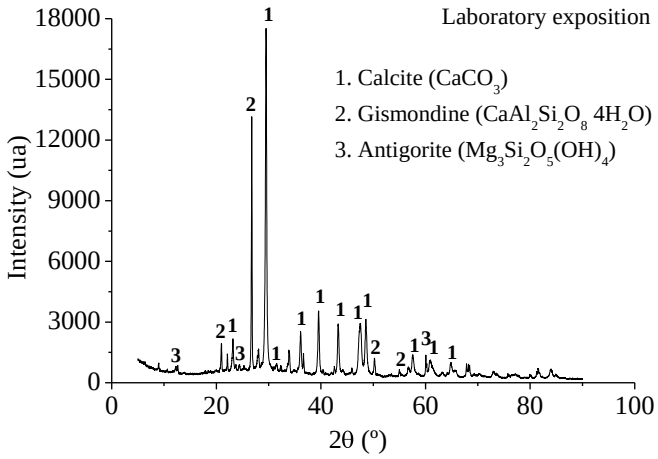

FIGURE 6 – X-RAY DIFFRACTION PATTERN OF THE TILE AGED IN THE LABORATORY.

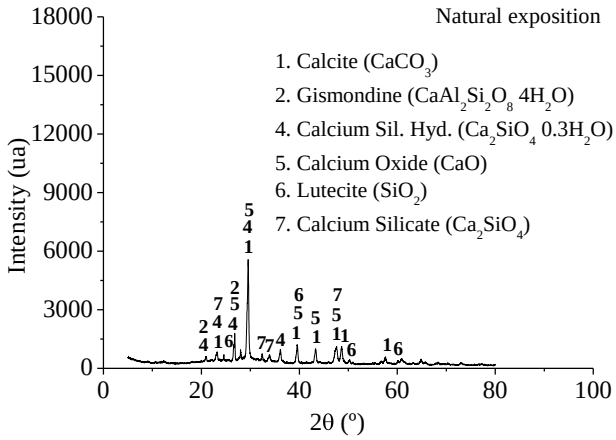

FIGURE 7 – X-RAY DIFFRACTION PATTERN OF THE TILE AGED UNDER WEATHERING EXPOSITION.

Diffuse peaks at 48.6º, 47.6º and 47.3º of both aged in laboratory and under weathering exposition, similarly to those reported by Cole & Kroone [22] confirmed the presence of poorly crystallized calcite. Anhydrous calcium silicate peaks were only found in the weathering exposed tile, showing that the matrix of this sample had

not yet completely hydrated. The main peak of C–S–H (29.5°) is coincident with the main peak of calcite and calcium oxide in the specimen aged under weathering exposition. Peaks of high Ca/Si C–S–H [23] do not appear in the weathering exposed tile.

Some cementitious phases (antigorite and gismondine) identified in the x-ray of the laboratory cured tiles seem to be less stable in contact with the rainwater than calcite for example

Figures 8 and 9 present TG, DSC and DTG curves from specimens of laboratory and weathering exposition, respectively. Table 6 depicts the weight losses from the TG tests, expressed as a percentage of total fractions. The main compounds that decompose thermally up to 350°C (1st peak) are C–S–H, ettringite and gypsum [24,25], however this last two minerals were not identified in X-ray diffraction. From about 350 to 450°C (2nd peak), thermal decomposition of magnesium compounds takes place [17].

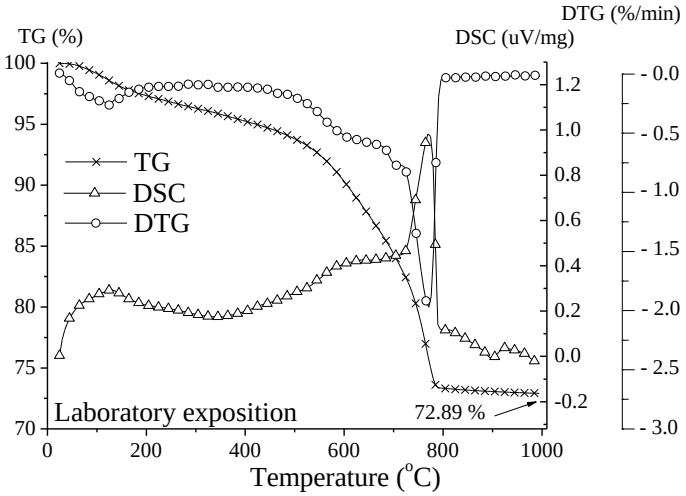

FIGURE 8 – TG, DSC AND DTG CURVES OF THE TILES AGED IN THE LABORATORY.

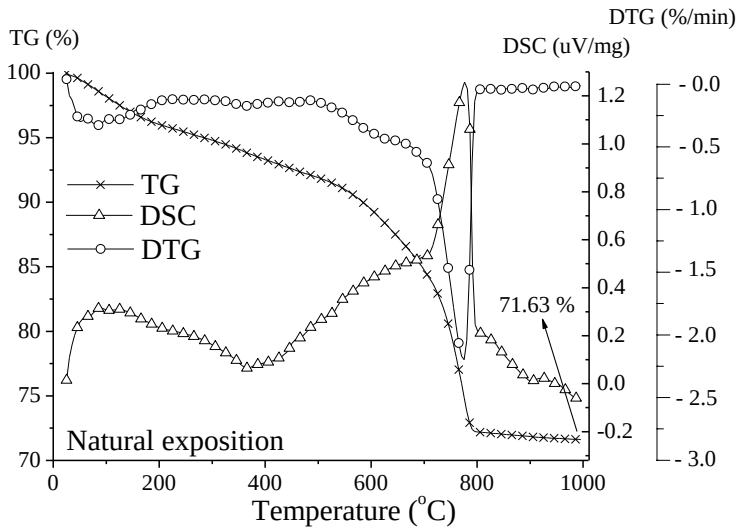

FIGURE 9 – TG, DSC AND DTG CURVES OF THE TILES AGED UNDER WEATHERING EXPOSITION.

As presented in the Table 6 the amount of magnesium compounds in the tiles aged in laboratory was higher than that in tiles under weathering exposition, which is in accordance with the absence of Mg phases in the X-ray diffraction pattern of the weathering exposed tile. Portlandite was not identified in the X-ray diffraction. However in the TG analyses the onset of an endotherm at about 450°C is due to the $Ca(OH)_2$ formed from the further hydration of the C3S phase [26] in the tile under weathering exposition (Figure 9). Thermal decomposition of poorly crystallized calcite [22] occurs in the range between 500 and 800°C [27] and by well-crystallized calcite at temperatures above 800°C [23,28].

TABLE 6 – LOSS OF WEIGHT ON TG ANALYSES.

	Laboratory exposition	Weathering exposition
	Weight loss (%)	
C-S-H and sulfoaluminates	5.06 ± 1.36	5.82 ± 0.12
Magnesium compounds	1.68 ± 0.62	1.31 ± 0.30
Portlandite	0.74 ± 0.14	0.79 ± 0.16
Poorly crystallized carbonates	19.16 ± 1.88	20.44 ± 1.05
Well-crystallized calcite	0.56 ± 0.21	0.53 ± 0.07

The C–S–H halo in laboratory exposition is less intense than the halos of weathering exposition. This relates to an increase in the amount of C–S–H when in contact with rainwater (exposition to weathering). Calcium sulphate dehydrate was not detected in the samples. The presence of calcium sulphate dehydrate is associated to ettringite carbonation reaction [17].

CONCLUSIONS

Based on the testing results, it may be concluded that:

The increase of the water absorption and apparent void volume in the roofing tiles aged under weathering exposition could be the consequence of the leaching of some less stable cementitious products, which decreased the bulk density of the specimens.

Weathering exposed tile revealed a coarsening of pores greater than 100 nm in comparison with the tile aged in laboratory. Coarsening has been associated to the SiO_2 (gel) formation during carbonation of C–S–H and leaching of the cement matrix. During the weathering exposition the continuous hydration of cement occurred and led to the reduction of the matrix voids.

In the tiles aged under weathering exposition, Calcium hydroxide ($Ca(OH)_2$) was not identified. In both tiles (in the laboratory and under weathering exposition) occurred adsorption of CO_2 in the cement based matrix and formation of calcite ($CaCO_3$).

ACKNOWLEDGMENT

The authors were supported by grants offered by CNPq, Capes and Fapesp, Brazil, and by Colciencias and the Ministery of Agriculture and Rural Development, Colombia.

REFERENCES

1. Soroushian, P. and Marikunte S., “High Performance Cellulose Fiber Reinforced Cement Composites,” *Proceedings of the international workshop “High Performance Fiber Reinforced Cement Composites*, RILEM, E&FN SPON, 1992.
2. Portland Cement Association. “Fiber Reinforced Concrete”, *PCA*, 1991, 48p.

3. Coutts R. S. P. A review of Australian research into natural fibre cement composites Cement and Concrete Composites, 2005, 27 (5), 518-526.
4. Swamy, R. N.. Influence of slow crack growth on the fracture resistance of fibre cement composites. The International Journal of Cement Composites, 1980, 2 (1), 43-53.
5. Gutierrez, de R., Delvasto, S., "Cabuya in cement composites", Ceramic Matrix Composites and Other Systems. *Proceedings of the Ninth International Conference on Composite Materials (ICCM/9)*. University of Zaragoza, Spain, 1993, 834-841.
6. Alban, F., "Cabuya fiber mortar for corrugated tiles and flat sheets," Ceramic Matrix Composites and Other Systems. *Proceedings of the Ninth International Conference on Composite Materials (ICCM/9)* University of Zaragoza, Spain, 1993, pp. 830-833.
7. Savastano Jr. H., Agopyan V., Nolasco A. M., Pimentel L. Plant fibre reinforced cement components for roofing Construction and Building Materials, 1999 ,13 (8), 433-438.
8. Gutierrez, R. M., Lopez, M., Delvasto, S, "Desarrollo de elementos de construccion reforzados con fibra de fique" *Proceedings of ARQUIMACON 96*, Sevilla, Spain, 1996.
9. Delvasto,S. Gutiérrez R.M., Escándon A. M. Mechanical Properties of Polymer Portland Cement Concretes Reinforced With Steel, Polypropylene, and Fique Fibers, *Proceedings IAC-NOMAT*, Joao Pessoa, Brazil, 2003.
10. Delvasto, S., Gutiérrez R. M., Váldez Y. Comparative study of the pull-out behavior of Fique fibers in mortars of portland cement. In: *Conferência Brasileira de Materiais e Tecnologia Não-Convencionais: Habitações e Infra-estrutura de Interesse Social – Brasil NOCMAT 2004.* Pirassununga. Anais… Pirassununga: FZEA-USP, 2004 (CD-ROM. Pirassununga - SP, Brasil, 2004).
11. Kuder, K. G., Shah S. P. Effects of pressure on resistence to freezing and thawing of fiber-reinforced cement board. ACI Materials Journal. 2003, 463-468.
12. Nita, C.; John, V. M.; Dias, C. M. R.; Savastano Jr., H.; Takeashi, M. S. In Effect of metakaolin on the performance of PVA and cellulose fibers reinforced cement. *Proceedings of 17th ASCE Engineering Mechanics Conference*, University of Delaware, Newark, DE, 2004, 11p
13. Mehta, P. K.; Monteiro, P. J. M. Concrete: Microstructure, Properties, and

Materials; 3rd ed., McGraw Hill: New York, USA, 2006, 659p.

14. Innocentini, M. D. M., Pardo, A. R. F., Pandolfelli, V. C. Modified Pressure–Decay Technique for Evaluating Highly Dense Refractories Permeability, J. Am. Ceram. Soc., 2000, 83 (1), 220–222.
15. Innocentini, M. D. M., Pardo, A. R. F., Menegazzo, B. A., Bittencourt, L. R. M., Rettore, R. P., Pandolfelli, V. C. Permeability of high-alumina refractory castables based on various hydraulic binders. J. Am. Ceram. Soc., 2002, 85 (6), 1517–1521.
16. Salomão, R., Cardoso F. A., Innocentini1, M. D. M., Bittencourt, L. R. M., and Pandolfelli, V. C. 2003. Polymeric fibers and the permeability of refractory castables. Cerâmica 49; 23-28 [in Portuguese].
17. Dias CMR, Cincotto MA, Savastano Jr. H, John VM. Long-term aging of fiber-cement corrugated sheets – The effect of carbonation, leaching and acid rain, Cement and Concrete Composites 2008, 30 (4), 255-265.
18. Bier T. A., Kropp J, Hilsdorf H. K. Carbonation and realkalinization of concrete and hydrated cement paste. In: Durability of construction materials 3, *Proceedings of the 1st congress from materials science to construction materials engineering*, RILEM, 1987.
19. Haga K., Sutou S., Hironaga M., Tanaka S., Nagasaki S.. Effects of porosity on leaching of Ca from hardened ordinary Portland cement paste. Cement Concrete Research, 2005; 35(9), 1764–75.
20. Gram, H. E. 'Durability of natural fibres in concrete', in Swamy R N, Natural Fibre Reinforced Cement and Concrete (Concrete Technology and Design 5), Glasgow, Blackie, 1988, 142-172.
21. Ramakrishna, G., T. Sundararajan Studies on the durability of natural fibres and the effect of corroded fibres on the strength of mortar. Cement and Concrete Composites 2005, 27, 575–582.
22. Cole W. F., Kroone B. Carbon dioxide in hydrated Portland cement. J Am Concrete Inst. 1960, 31, 1275–1295.
23. Chen J. J., Thomas JJ, Taylor H. F. W, Jennings H. M. Solubility and structure of calcium silicate hydrate. Cement Concrete Res. 2004; 34(9):1499–519.
24. Taylor H. F. W. Editor. Cement chemistry. Thomas Telford; 1997.

25. Ramachandran V. S. Applications of differential thermal analysis in cement chemical. New York: Chemical Publishing Company; 1969.

26. Ramachandran, V. S. Handbook of analytical techniques in concrete science and technology Edited by Ramachandran V. S.and Beaudoin J. J. Noyes Publications,Park Ridge, New Jersey, U.S.A. William Andrew Publishing, LLC Norwich, New York, U.S.A. 1999. 964p.

27. Gualtieri A. F., Tartaglia, A. Thermal decomposition of asbestos and recycling in traditional ceramics. J. European Ceramic. Soc., 2000, 20 (9), 1409-1418.

28. Sato N.M.N. Porosity and mass transport on concrete [Thesis of Polytechnic School of University of São Paulo], São Paulo, 1998 [In Portuguese].